MCB
Journals.ASM.org

RNA Profiling and Chromatin Immunoprecipitation-Sequencing Reveal that PTF1a Stabilizes Pancreas Progenitor Identity via the Control of MNX1/HLXB9 and a Network of Other Transcription Factors

Nancy Thompson,[a] Emilie Gésina,[a] Peter Scheinert,[c] Philipp Bucher,[a,b] and Anne Grapin-Botton[a,d]

Swiss Institute for Experimental Cancer Research[a] and Swiss Institute of Bioinformatics,[b] Ecole Polytechnique Fédérale de Lausanne, 1015 Lausanne, Switzerland; AmpTec GmbH, 22767 Hamburg, Germany[c]; and DanStem, University of Copenhagen, Copenhagen, Denmark[d]

Pancreas development is initiated by the specification and expansion of a small group of endodermal cells. Several transcription factors are crucial for progenitor maintenance and expansion, but their interactions and the downstream targets mediating their activity are poorly understood. Among those factors, PTF1a, a basic helix-loop-helix (bHLH) transcription factor which controls pancreas exocrine cell differentiation, maintenance, and functionality, is also needed for the early specification of pancreas progenitors. We used RNA profiling and chromatin immunoprecipitation (ChIP) sequencing to identify a set of targets in pancreas progenitors. We demonstrate that *Mnx1*, a gene that is absolutely required in pancreas progenitors, is a major direct target of PTF1a and is regulated by a distant enhancer element. *Pdx1*, *Nkx6.1*, and *Onecut1* are also direct PTF1a targets whose expression is promoted by PTF1a. These proteins, most of which were previously shown to be necessary for pancreas bud maintenance or formation, form a transcription factor network that allows the maintenance of pancreas progenitors. In addition, we identify *Bmp7*, *Nr5a2*, *RhoV*, and *P2rx1* as new targets of PTF1a in pancreas progenitors.

Pancreatic transcription factor 1a (*Ptf1a*) encodes a basic helix-loop-helix (bHLH) transcription factor most closely related to the *Twist* subclass (31). It was first identified as one of three subunits of the PTF1 transcription factor complex that is required for the expression of pancreatic digestive enzyme genes (11, 53–55). The PTF1 complex also comprises a class A bHLH protein, p64, also known as PTF1b/TCF12/HEB and p75/TCF3/E12/E47, a subunit that is required for the import of the PTF1 complex into the cell nucleus (6, 60). In addition to this initially identified tripartite complex, PTF1 was also shown to interact with recombination signal binding protein for immunoglobulin kappa J region (RBPJ/RBPJK) or recombination signal binding protein for immunoglobulin kappa J region-like (RBPJL) depending on cell types and developmental stages (6, 39, 46). The PTF1 complex binds a bipartite cognate site that contains two distinct sequence motifs (11, 55). p64 was shown to contact a TGGGAAA/TTTCCCA sequence (A box/TC box), and although p64 was identified as HEB (NCBI), RBPJL and RBPJK subsequently were shown to bind this sequence (6, 39, 46). PTF1a binds to CANNTG, the canonical binding site for bHLH proteins (E box; formerly called B box) (11, 55). Interactions with NR5A2/LRH-1 also were recently uncovered (23).

PTF1a is a protein that is required for the differentiation of the nervous system (2, 18, 24, 50), retina (14, 15, 44), and pancreas. The truncation of the human *PTF1A* gene leads to permanent neonatal diabetes mellitus due to pancreas agenesis (58, 59, 62). In *Ptf1a* knockout (KO) mice, exocrine pancreas agenesis was similarly observed (29, 32). Although the expression of this gene was initially thought to be limited to exocrine cells (32), tracing experiments have clearly shown that it is also expressed in early pancreas progenitors that give rise to exocrine and endocrine cells, including insulin-secreting beta cells (9, 16, 29). This is further supported by the reduction in endocrine cell numbers in the absence of PTF1a in mice and zebrafish (16, 29, 38). In the absence of PTF1a, cells of the pancreatic bud stop proliferating at embryonic day 10.5 (E10.5) and adopt a duodenal fate (16, 29). Experiments manipulating the dosage of PTF1a in zebrafish and mice show that low levels of PTF1a are necessary in pancreas progenitors, whereas high levels are needed for exocrine differentiation (13, 16). Moreover, elegant experiments, including the generation of mutants harboring specific point mutations preventing interaction with RBPJL but not RBPJ, demonstrated that the function of PTF1a in the exocrine program induction relies mostly on RBPJL (40), whereas its early activity in pancreas progenitor maintenance depends on RBPJK (39). Lastly, the gain of function of PTF1a in *Xenopus* expands pancreas formation in the foregut in sites of pancreatic duodenal homeobox 1 (PDX1) expression (1, 27). Although several targets of PTF1a in exocrine cell differentiation were clearly established (11, 40), very few targets acting in early pancreas progenitors have been identified (63). To identify such targets, we compared the mRNAs differentially regulated in E10.5 pancreas progenitors in *Ptf1a* KOs to those of controls and we conducted chromatin immunoprecipitations (ChIPs) of PTF1a to identify direct targets.

Received 26 September 2011 **Returned for modification** 26 October 2011
Accepted 29 December 2011
Published ahead of print 9 January 2012
Address correspondence to Anne Grapin-Botton, anne.grapin-botton@epfl.ch.
Supplemental material for this article may be found at http://mcb.asm.org/.

doi:10.1128/MCB.06318-11

MATERIALS AND METHODS

Animals. *Ptf1a* mutant mice (MGI 1328312) were generated by gene targeting as previously described (32). Embryos were collected at indicated times; midday on the day of vaginal plug appearance was considered E0.5. DNA isolated from embryonic tissue or tail biopsy specimens was used for genotyping; primers are listed in Table S4 in the supplemental material. To test the activity of the *Mnx1* 5′ flanking sequence in the pancreas of transgenic mice, we cloned an 8-kb promoter (Ch5: 29804983 to 29813141) and an 11-kb promoter (Ch5: 29804983 to 29815469) upstream of a LacZ reporter. The 212-kb Mnx1::LacZ reporter mouse was constructed by chromosomal engineering in *Escherichia coli* EL250. The bacterial artificial chromosome (BAC) RP24-548M16 (AC164700) was used as a source for the *Mnx1* gene. The targeting vector was constructed by inserting a LacZ FLP recombination target (FRT) AMP cassette just before the ATG of *Mnx1* (unpublished data). Each recombinant plasmid was microinjected into pronuclei of fertilized eggs.

cDNA profiling. Dorsal pancreatic E10.5 anlagen (500 to 1,000 cells) were homogenized, and RNA was purified using the RNeasy minikit (Qiagen) including on-column DNase treatment (Qiagen). RNA yields were about 5 ng from 3 dorsal buds. For microarray profiling, cDNA with a T7 promoter incorporated was generated and two amplification rounds were performed (AmpTec, ExpressArt mRNA amplification kit) (Fig. 1A). In the second round, the template DNA was transcribed *in vitro* using the IVT labeling kit (Affymetrix); cRNA was purified, quantified, and fragmented. Two $Ptf1a^{+/-}$ and three $Ptf1a^{-/-}$ cRNA samples passed quality controls and were hybridized to Affymetrix Gene Chip Mouse Genome 430 2.0 arrays. GCOS (GeneChip Operating Software) was used to convert CEL files to CHP files. RACE (remote analysis computation for gene expression) (52), based on RMA in Bioconductor, was used for normalization, quality control and gene expression levels. Gene Ontology (GO) category enrichment was analyzed using David v6.7 (http://david.abcc.ncifcrf.gov/home.jsp) (12).

Quantitative reverse transcription-PCR (qRT-PCR) samples are identified in the specific figure legends. TaqMan probes and SYBR primers are detailed in Table S4 in the supplemental material. TaqMan Gene Expression Master Mix or Power SYBR green PCR Master Mix (AB) was used with a Step One Plus qPCR machine (AB).

Whole-mount immunofluorescence, immunohistochemistry, and β-galactosidase staining. For whole-mount immunofluorescence, embryos were fixed in 4% paraformaldehyde for 1 h at room temperature and dehydrated. Tissues were rehydrated and incubated in PGTA (0.2% gelatin, 1.6% blocking, 16% sheep serum, 0.25% Triton X-100, and 0.1% azide in phosphate-buffered saline [PBS]) with rabbit anti-Pdx1 antibody (a gift from Chris Wright) for 48 h at 4°C followed by overnight incubation with donkey anti-rabbit IgG–Alexa Fluor 488 (Invitrogen). LacZ expression was visualized in whole mounts by 5-bromo-4-chloro-3-indolyl-β-D-galactosidase staining at 37°C after fixation for 30 min. Images were taken with a Leica MZ 16 1FA Stereomicroscope.

For immunohistochemistry, fixed embryos were washed with PBS, equilibrated in 15% sucrose-PBS overnight, and embedded in 30% gelatin. Eight-micrometer sections were collected and stained with indicated antibodies (see Table S4 in the supplemental material) overnight at 4°C. Nuclei were counterstained with 4′,6-diamidino-2-phenylindole (DAPI; Sigma). A Zeiss Axioplan 2 microscope was used for image acquisition with a Zeiss AxioCam MRm B/M.

Chromatin immunoprecipitation. 266-6 cells (ATCC CRL-2151) were grown in DMEM (Invitrogen)–10% fetal calf serum and passaged twice per week (49). For ChIP, cells between passages 26 and 30 were chemically cross-linked by removing the media, adding 1% formaldehyde in DMEM to the cells, and incubating for 10 min at room temperature. The fixed cells were washed once with PBS and then incubated with 125 mM glycine in PBS for 5 min. The cells were rinsed with PBS and then collected by scraping in PBS. Cells were washed once with PBS and protease cocktail inhibitors (Roche); the cell pellet was flash frozen and stored at −80°C with the cell count noted.

Chromatin was extracted from 20×10^7 266-6 cells as described in reference 37 in 30 ml lysis buffer 1, 24 ml lysis buffer 2; after centrifugation the pellet was taken up in 4.5 ml lysis buffer 3. The chromatin was divided into 4 aliquots in 15-ml conical centrifuge tubes and fragmented into 100- to 500-bp fragments with 65 cycles of 30 s on/30 s off at 4°C using a Biorupter UCD-300 (Diagenode). The fragmented chromatin was centrifuged for 10 min at $12{,}000 \times g$ to remove cell debris. The supernatant was used immediately for immunoprecipitations.

For each experiment the following antibodies were used: IgG as a negative control (Bethyl), RNA polymerase II 8WG16 as a positive control (Covance), and Ptf1a (Beta Cell Biology Consortium) in duplicate. Each antibody was precoupled to 5 mg/ml bovine serum albumin (BSA) in PBS with prewashed 50 μl protein A plus 50 μl protein G Dynabeads (Invitrogen). In a 1.5-ml smooth-walled centrifuge tube, 1 ml of cleared chromatin was added to 100 μl of beads/antibody and 300 μl of a solution containing 1% Triton X-100, 0.1% deoxycholate (DOC), 1× protease inhibitors, and Tris-EDTA (TE). This was turned for 16 h at 4°C. The beads/chromatin/antibody complex was recovered using a magnet; beads were washed 20× with 1 ml RIPA buffer (50 mM HEPES, pH 7.6, 500 mM LiCl, 1 mM EDTA, 0.7% DOC, 1% NP-40) with a final wash of TE. The chromatin was eluted with 100 μl warm TE–1% SDS and diluted with 100 μl TE and was reverse cross-linked by adding 2 μl 5 M NaCl and incubating overnight at 65°C. One percent of the input chromatin (10 μl) was taken up to 200 μl TE and reverse cross-linked as the IP. The DNA was incubated for 60 min with RNase A followed by proteinase K treatment for 2 h. The ChIPed DNA was purified on a QIAquick PCR purification column (Qiagen). The DNA was eluted with 2× 50 μl elution buffer and used directly for quantitative PCR (QPCR) or ChIP sequencing (ChIP-Seq). Sequencing libraries from Ptf1a chromatin immunoprecipitation products and 226-6 cell purified input chromatin were prepared using the ChIP-Seq sample preparation kit (Illumina no. IP-102-1001) according to the protocol supplied with the reagents and using 5 ng of ChIP sample quantified using the Qubit fluorometer (Invitrogen). One lane of each library was sequenced on the Illumina genome analyzer IIx using the Single-Read cluster generation kit v4 and 36 cycle sequencing kit v4.

ChIP-Seq data analysis. Data were processed with the Illumina Pipeline software v1.60. The sequence reads were mapped to the mouse genome assembly NCB37/mm9 with the Eland program allowing for up to two mismatches. Downstream analysis was carried out with the ChIP-Seq tools (web access at http://ccg.vital-it.ch/chipseq/, source code download from http://sourceforge.net/projects/chip-seq/). For a detailed description of these methods, we refer to our previous paper on STAT1 ChIP-Seq data (57). Overall, we followed the same protocol as described previously. The Eland output was first converted into SGA, the input format required by the ChIP-Seq tools. Note that in the SGA format, a tag is represented by a single genomic position corresponding to the 5′ end of the sequence read. With the aid of the ChIP-Cor program, we then determined the average shift between 5′ and 3′ tags in the peak regions, which turned out to be 150 bp. Based on this result, we "centered" all tags by 75 bp, i.e., we shifted the tags mapping to the + or − strand by 75 bp downstream or upstream, respectively. Centering was applied prior to all analysis steps described further below.

For data viewing in a UCSC genome browser environment, we generated a BigWig file (30) with 50-bp resolution from the centered tag distributions. For peak extraction we used the ChIP-peak tool with the following parameter settings: window width, 200; vicinity range, 200; peak threshold, 20; count cutoff, 1; peak refinement on; Repeat Masker on. The ChIP-Peak program uses a sliding window approach and returns the center positions of the windows that have at least a threshold number of tags and are maximal within an area of the size defined by the vicinity range parameter. Setting the count cutoff value to 1 has the consequence that multiple tags mapping to exactly the same positions are counted only once. Repeat masking restricts peak finding to the nonrepetitive part of the genome, as defined by the RepeatMasker track of the UCSC genome browser.

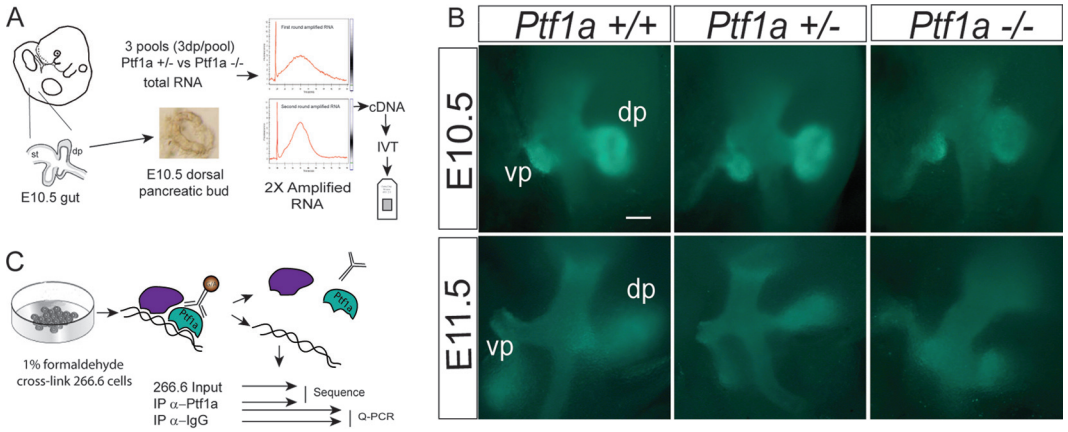

FIG 1 Experimental flow charts and starting material. (A) For RNA profiling, the E10.5 pancreatic bud epithelia were mechanically dissected, and RNA was extracted from three pools of three buds from each genotype. The RNA was twice linearly amplified and then reverse transcribed, and RNA probes were generated for hybridization in triplicate to Affymetrix GeneChip Mouse Genome 430 2.0. (B) Whole-mount immunocytochemistry for PDX1 showing high PDX1 expression in the dorsal (dp) and ventral (vp) pancreatic buds at E10.5 (upper panels). Expression is lower in the PTF1a KO mouse. Expression between the buds is in the duodenum (bottom), and the antral stomach (top) serves as a reference for expression unaffected by PTF1a. The bottom panels show a decrease in PDX1 levels at E11.5 in the WT and a collapse of dorsal pancreatic bud in the KO. All pictures were captured with the same exposure time. Scale bar, 200 μm. (C) For ChIP, 266-6 cells were cross-linked, sheared, and immunoprecipitated with anti-PTF1a or control anti-IgG antibodies. Immunoprecipitated chromatin and control input were sequenced at high throughput. A subset of potential binding sites was confirmed by QPCR comparing chromatin precipitated by anti-PTF1a and anti-IgG antibodies.

The false discovery rate at peak threshold 20 was estimated by extracting peaks at an equivalent threshold from the input control sample. The nontrivial issue is how to define an equivalent threshold. We opted for the following method. We first determined the average tag content in a window of 200 bp in the part of the genome to which tags can be mapped uniquely. These numbers turned out to be 2.678 and 2.334 for the input and ChIP samples, respectively. For the ChIP-Seq experiment, the probability of finding 20 or more tags in a window of 200 bp was then estimated to be 1.1×10^{-13} assuming a Poisson distribution. This probability is best matched by a threshold of 21 tags for the input control sample corresponding to a probability of 1.8×10^{-13}.

The transcription start site (TSS) list used for analyzing the distribution of Ptf1a peaks around promoters was downloaded from the UCSC genome browser database with the aid of the "Table Browser." As TSS position, we used the txStart field from the "UCSC Genes" track. As gene identifiers we used the linked geneSymbol field from the kgXref table. The gene list was made nonredundant by retaining only the most upstream TSS from groups of gene entries sharing the same gene symbol.

Binding sites were identified using MatInspector.

ChIP-QPCR analysis of ChIP-Seq targets. To confirm the Ptf1a peaks from the ChIP-Seq data set, we did quantitative PCR using Power SYBR Green Master Mix (AB) with 5-μm oligonucleotides (see Table S4 in the supplemental material) in an Applied Biosystems StepOnePlus PCR machine. A standard curve was created from the INPUT 266-6 purified chromatin for each primer pair. Immunopreciptated Ptf1a and IgG samples were quantified as well as control regions for each gene.

Luciferase reporter constructs and assays. Luciferase reporter plasmids were generated by PCR from the BAC RP24-548M16 for the proximal promoter of Mnx1/Hlxb9 (kb −1.19 NheI site to +193 in the 5′ UT) and cloned into the NheI/XhoI sites of pGL3 Basic (Promega). The two major Ptf1a binding sites at kb −51.8 and −44.8 were amplified by PCR from the above BAC and inserted upstream individually at the MluI 5′ and NheI 3′ sites in the Mnx1 pGL3 construct. Site-directed mutagenesis of the kb −51.8 element was done by overlapping extension PCR. The E box, the binding site for Ptf1a, was mutated to a PacI site (CAGCTG to TAATTA). *Pfu* polymerase (Stratagene) was used for all PCRs. All oligonucleotides are provided in Table S4 in the supplemental material. For luciferase assays, 4×10^5/well 266-6 cells were plated in a 24-well plate 16 h before transfection. One microgram DNA per well consisting of 0.8 μg of either the pGL3 basic or Mnx1-pGL3 constructs described above, 0.2 μg of pCIG (green fluorescent protein [GFP]), and 3 ng of TK *Renilla* luciferase were transfected with 3 μl of X-tremeGene (Roche) and repeated in triplicate. Passive lysis buffer (PLB) and the dual luciferase reporter kit (Promega) were used to measure firefly and *Renilla* luciferase activities.

BrdU incorporation experiments. For bromodeoxyuridine (BrdU) labeling of embryos, pregnant mice were injected intraperitoneally with 1 mg/20 g body weight of BrdU (Sigma) in PBS 2 h before sacrifice.

ISH. *In situ* hybridizations (ISHs) were performed on 7-μm paraffin sections using a standard protocol. Briefly, sections were dewaxed and rehydrated prior to successive permeabilization with 0.2 N HCl (15 min; room temperature [RT]) and 10 μg/ml proteinase K (10 min; 37°C). Sections were further postfixed with 4% paraformaldehyde (10 min; RT) and treated with 0.6% acetic anhydride in 1.3% triethanolamine solution (pH 8). Prehybridization was then performed for 2 h in a 70°C hybridization oven in a chamber humidified with a 5× SSC (1 × SSC is 0.15 M Nacl plus 0.015 M sodium citrate)–50% formamide solution. The hybridization solution used was composed of 50% formamide, 5× SSC, pH 4.5, 2% blocking reagent (Roche), 5 mM EDTA, 0.05% CHAPS {3-[(3-cholamidopropyl)-dimethylammonio]-1-propanesulfonate}, 50 μg/ml heparin, 1 μg/ml yeast total RNA. Digoxigenin-labeled probes were diluted in the hybridization solution at a 1-μg/ml concentration, added to slides, and incubated overnight at 70°C. The next day slides were washed three times in 50% formamide–2× SSC at 65°C prior to immunodetection with an alkaline phosphatase-conjugated antidigoxigenin antibody (sheep; 1/2,000; Roche). Staining was performed using nitroblue tetrazolium (NBT)–5-bromo-4-chloro-3-indolylphosphate (BCIP) solution. A Leica DM5500B microscope equipped with a DFC 320 color camera was used for image acquisition.

RESULTS

A whole-genome approach to identify PTF1a targets in pancreatic progenitors. In order to determine PTF1a targets mediating pancreas progenitor maintenance and expansion, we used Affymetrix microarrays to identify mRNAs whose expression levels differed between heterozygous and homozygous null mutants for *Ptf1a* (32) (Fig. 1A). We observed that the pancreatic bud had a normal size and shape in *Ptf1a* knockouts (KOs) at E10.5 but at

E11.5 was smaller than age-matched heterozygous (HT) and wild-type (WT) controls (Fig. 1B). Thus, we dissected dorsal pancreatic buds at E10.5. Three pools of three pancreatic buds of the same genotype were used for RNA extraction, linear amplification (Fig. 1A), and hybridization to 6 Affymetrix GeneChip Mouse Genome 430 2.0 representing 34,000 genes. After quality checks and statistical analysis, 297 probe sets were more than 2.8-fold ($2^{-1.5}$) downregulated in the KO (see Table S1A in the supplemental material shows the first 100) and 275 probe sets had more than a 2.8-fold upregulation in the KO (see Table S1B in the supplemental material shows the first 100) at $P < 0.05$.

We found that *Ptf1a* itself was 7-fold decreased in *Ptf1a* KOs compared to heterozygotes. Validation by quantitative PCR confirmed a 5- and 7-fold reduction compared to HT and WT, respectively (data not shown). *Carboxypeptidase A1* (*Cpa1*) is the only exocrine enzyme gene expressed in pancreatic progenitors at E10.5 (see Fig. S1A in the supplemental material) and is under the transcriptional control of PTF1 in exocrine cells (11). It was 838-fold decreased in the KO. Validation by quantitative RT-PCR showed that the level in the KO was reduced by 99% compared to *Ptf1a*$^{+/-}$ pancreata (see Fig. S1B).

In parallel we conducted chromatin immunoprecipitation (ChIP) followed by high-throughput sequencing (ChIP-Seq) to determine the direct targets of PTF1a (Fig. 1C). Pancreatic buds at E10.5 contain only 500 to 1,000 cells and our attempt to perform ChIP-Seq from 300 pancreatic buds, at this stage failed. We therefore used the 266-6 pancreatic cell line as a model for PTF1a DNA binding in progenitors. 266-6 cells do indeed express PTF1a at levels similar to E10.5 pancreatic buds, and although they were originally derived from an acinar cell carcinoma, we found that they efficiently express numerous progenitor markers such as PDX1, HLXB9, OC1, and, to a lesser extent, NKX6.1 (see Fig. S2 in the supplemental material). The low expression levels of carboxypeptidase A are close to those found in E10.5 pancreatic buds and much lower than in adult exocrine cells (see Fig. S2 in the supplemental material). This expression profile highlights similarities with early pancreas progenitors (65). Among the PTF1a cofactors, they express high levels of RBPJ and low levels of RBPJL, consistent with their being closer to multipotent pancreas progenitors than to exocrine cells (see Fig. S2 in the supplemental material) (39, 40). This also shows that the PTF1 complex present in 266-6 cells should have a binding specificity more representative of early progenitors than of exocrine cells. ChIP-Seq was performed with an anti-PTF1a antibody (20) and yielded 24.6×10^6 sequence tags that could uniquely be mapped to the mouse genome assembly NCBI37/mm9. An input control sample produced 27.9×10^6 mappable tags. From these data, we were able to extract more than 30,000 peaks at an estimated false discovery rate of 6.7%. The genomic locations of the 936 strongest peaks covered by 200 or more sequence reads are given in Table S2 in the supplemental material, along with the names of the neighboring genes. Eighty-three percent of these sites harbored consensus E-box and A/TC-boxes, suggesting that it is unlikely that PTF1a binds DNA in the absence of an A/TC-box binding partner. The E-box and RBPJ binding sequences were 1, 2, or, more surprisingly, 3 helix turns apart. Based on the number of peaks identified, it can be argued that not all binding peaks regulate gene expression in progenitors or in 266-6 cells. However, the strong binding peaks (>100 tags) were found to be greatly enriched in the vicinity of the genes (±50 kb from start site) that are downregulated in *Ptf1a* KO cells (Fig. 2). Of the 78 genes corresponding to the 100 most downregulated probe sets in *Ptf1a* KO (see Table S1A in the supplemental material), 41% colocalize with a strong binding site according to the above criteria (see Table S3 in the supplemental material). This fraction goes down to 14% for the upregulated genes in *Ptf1a* KO (see Table S1B) and to 18% for all other (nonregulated) genes. Taking 18% as the false-positive rate and assuming that all downregulated genes that colocalize with a PTF1a site are direct targets, we estimate the fraction of direct targets to be 28% ($0.28 \times 100\% + 0.72 \times 18.2\% = 41\%$ as observed). Different simulations based on different thresholds of downregulation or peak calling as proposed in Table S3 give estimations of direct targets ranging from 17% to 36%. Among the direct targets reported in the work of Masui et al. in mature exocrine cells, 31 of 45 genes also had at least one peak in our study (40). Peaks were found up to 50 kb upstream and 100 kb downstream of transcription start sites, including in introns and exons. For *Ptf1a* and *Cpa1*, two known direct targets of *Ptf1a*, clear binding peaks were found. For *Cpa1*, a single high peak was identified by ChIP-Seq (see Fig. S1C) encompassing 3 PTF1a conserved binding sequences confirmed by ChIP-PCR. The first one between +141 and +159 (area I; see Fig. S1C) corresponds to the binding site previously identified by DNase footprinting (11). In addition, two new tandem sites between bp −23 and +24 were identified (area II; see Fig. S1C). For Ptf1a, a small binding peak upstream was identified that corresponds to the previously identified binding site (41) and an additional one with more tags was uncovered 40 kb downstream (see Table S2). Taken together, these experiments reveal the structure of binding sequences, confirming that consensus E-box and A/TC-box can be 1 and 2 helix turns apart, but we also unexpectedly identified consensus sequences 3 helix turns apart. The two motifs with constrained spacing have a remarkably high binding prediction power; 50% of them are located in peaks.

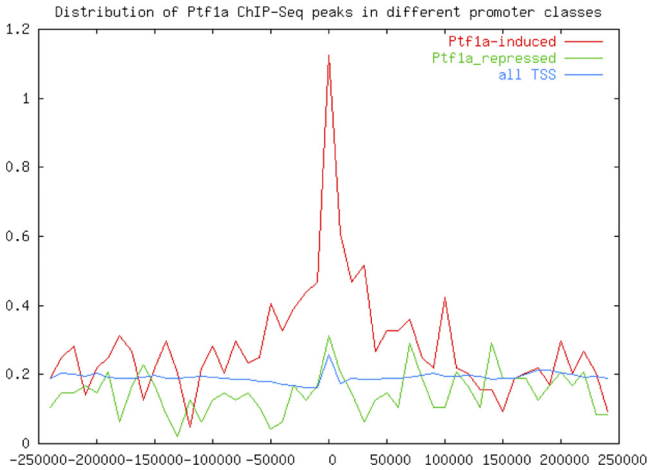

FIG 2 Distribution of Ptf1a ChIP-Seq peaks in transcriptionally regulated versus nonregulated genes. The *x* axis shows the base distance from the most upstream transcription start site, noted as 0. The *y* axis is the number of peaks of more than 20 tags per 10-kb interval. The red line shows that for genes that depend on PTF1a for their expression in pancreas progenitors, binding peaks are enriched from kb −50 to kb +100 around the start site compared to genes repressed by PTF1a (green line) or random genes (blue line) which had no peak enrichment.

Four transcription factors essential for pancreas progenitor maintenance are controlled by PTF1a. In spite of the high num-

bers of direct targets, only a few transcription factors potentially relaying PTF1a activity were identified: *Motor neuron and pancreas homeobox 1* (*Mnx1/Hlxb9*) (67-fold downregulated in *Ptf1a* KO), *Pancreatic and duodenal homeobox 1* (*Pdx1*) (4-fold), *NK6 homeobox 1* (*Nkx6.1*) (4-fold) and *One cut domain, family member 1* (*Onecut1/Hnf6*) (4-fold). No Gene Ontology category as a whole was significantly enriched with a P value lower than 10^{-3}, although pancreas development genes and transcription factors were slightly enriched among genes downregulated in *Ptf1a* KO ($P = 1.3 \times 10^{-3}$ and 3.5×10^{-3}, respectively). In particular, although the null pancreatic buds do not expand normally after E10.5 (16) (see Fig. S3 in the supplemental material), the cell cycle and apoptosis Gene Ontology categories were not changed significantly ($P < 10^{-3}$). qRT-PCR experiments at E10.5 confirmed that *Mnx1* was diminished 32-fold in *Ptf1a* KO compared to WT and 21-fold compared to heterozygotes, suggesting a dosage dependency (Fig. 3). *Pdx1*, *Nkx6.1*, and *Onecut1* were respectively also reduced, often in a dose-dependent manner although less drastically, and they are coexpressed with PTF1a at E10.5 (Fig. 3) (20). As downregulation may be due to either a decrease of expression in all cells or a decrease in the number of cells expressing MNX1, we carried out immunohistochemistry for this protein in *Ptf1a* KOs. Although no difference in MNX1 expression was detected at E9.5 in different *Ptf1a* genotypes, at E10.5 there was a decrease in heterozygotes and no detectable levels in homozygous null mutants (Fig. 4A). This suggests that MNX1 requires PTF1a for its maintenance rather than for its initial expression. Four PTF1a-binding peaks were identified between 28.6 and 51.8 kb upstream of Mnx1 (Fig. 3). Enrichment of PTF1a was confirmed at all four locations by ChIP-PCR, with greater binding at kb −44.8 and kb 51.8 sites than at kb −28.6 and −37.5, and a consensus sequence for PTF1 (A/TC and E box) was identified at these four sites. PDX1 levels in the pancreas of *Ptf1a* KOs were reduced at E10.5 to close to the low expression levels found in the duodenum (Fig. 1B), in agreement with previous observations (16, 42, 63). A strong PTF1a-binding peak covering an A/TC- and E-box was identified 2.4 kb upstream of Pdx1, in the region known as area III (Fig. 3), as expected from previous work (16, 42, 63) In addition, another peak was identified 40 kb downstream. Two PTF1a-binding peaks were identified at 70 kb upstream of *Nkx6.1* and 75 kb downstream (Fig. 3). Both were confirmed by QPCR (Fig. 3) and harbored the dual PTF1 binding sequences. Three PTF1a-binding peaks were identified at 6 kb upstream of *OC1*, in the intron, and 23 kb downstream (Fig. 3). All were confirmed by QPCR. We also observed that some genes were upregulated in *Ptf1a* KOs, among which was *Foxa1*. Although inactivation data demonstrate a function for FOXA1 in the pancreas (17), our *in situ* hybridization shows that the expression levels are very low at E10.5 and E14.5 in the pancreas whereas robust expression levels were detected in the duodenum and stomach (see Fig. S4 in the supplemental material). In *Ptf1a* KOs, *Foxa1* became detectable in the pancreas at levels similar to those in the duodenum (see Fig. S4), suggesting that pancreatic buds acquire a duodenal character. *Foxa1* upregulation in the *Ptf1a* KO was confirmed by qRT-PCR (see Fig. S4). This observation is in line with previous findings that large numbers of cells that had begun to enter a pancreatic program are later found in the duodenum of *Ptf1a* KOs (29), adopting normal intestinal fates. Among the downregulated genes, PTF1a binding peaks were not detected, showing that PTF1a does not most likely act as a transcriptional repressor.

Mnx1, a major unexpected direct PTF1a target. *Mnx1* is the pancreas progenitor transcription factor that is the most highly downregulated in *Ptf1a* KOs. The absence of dorsal pancreatic bud in *Mnx1* KOs shows that this gene is crucial in pancreas development and could be a major mediator of PTF1a activity in progenitors (21, 35). Our experiments demonstrate that direct binding of PTF1a is detected at distant sites upstream of the *Mnx1* gene and may control its expression. The elements that control *Mnx1* expression in the motoneurons have been previously identified in its 9-kb 5′ promoter (4, 34). However, the sequences driving its expression in the pancreas have not been identified. We therefore generated transient transgenic embryos bearing 8-kb and 11-kb upstream Mnx1 promoters driving LacZ (Fig. 4B). Although 10 $LacZ^+$ embryos showed clear expression in the motoneurons, no expression was detected in the pancreas at E10.5 (Fig. 4C). We then inserted LacZ by homologous recombination at the ATG of a 212-kb BAC extending 80 kb upstream of the *Mnx1* start site, encompassing the whole gene and extending 120 kb 3′ (Fig. 4D). Two independent lines showed expression in the motoneurons but also in the entire dorsal gut tube and dorsal and ventral pancreas at E10.5 (Fig. 4E). These results are in agreement with the location of the four PTF1a binding sites identified by ChIP-Seq between kb −28.6 and −51.8. Pancreas regulatory sequences are either not located in the 11-kb proximal promoter or not sufficient for pancreas development. Binding sites for several other known pancreatic transcription factors are present within a few hundred base pairs of the kb −51.8 PTF1a binding site on the *Mnx1* promoter at increased frequency (see Fig. S5 in the supplemental material), suggesting that this may represent an enhancer element. The transcriptional activity of the two potential enhancers of *Mnx1* that bind PTF1a most efficiently (kb −44.8 and −51.8) was tested in 266-6 cells. Whereas a 1.4-kb minimal promoter of *Mnx1*, alone or in combination with the kb −44.8 element, drove minimal transcriptional activity in 266-6 cells, the 1.4-kb minimal promoter combined with the kb −51.8 element increased transcriptional activity 4-fold (Fig. 4F and G). Point mutations in the PTF1A consensus sequence suppressed this effect, indicating that this enhancer is active and dependent upon the PTF1A binding site (Fig. 4F and G). Taken together, these experiments show that PTF1a promotes *Mnx1* expression by directly binding to a distant enhancer at kb −51.8. This enhancer may be potentiated by several other binding sites between kb −28.6 and kb −51.8. Since *Mnx1* is required for pancreas progenitors to maintain their identity and expand, it may be a major mediator of PTF1a.

New PTF1a target genes. In addition to the genes with a known function in the pancreas, PTF1a-regulated genes of unknown function in this organ were identified in the RNA profiling experiments. Further validation by *in situ* hybridization was pursued on 14 genes that were downregulated in *Ptf1a* knockout and 4 that were upregulated (see Table S1 in the supplemental material). However, most were excluded due to low global or pancreatic signals. This led to the identification of 4 genes whose expression was detected in the E10.5 pancreas epithelium and was lost upon *Ptf1a* inactivation: ras homolog gene family, member V (RHOV) (436-fold decrease); purinergic receptor P2X, ligand-gated ion channel, 1 (P2RX1) (141-fold decrease); bone morphogenic protein 7 (BMP7) (4.8-fold decrease); and nuclear receptor subfamily 5, group A, member 2 (NR5A2) (4.7-fold decrease) (see Fig. 5A; see also Table S1A). These genes were also specifically

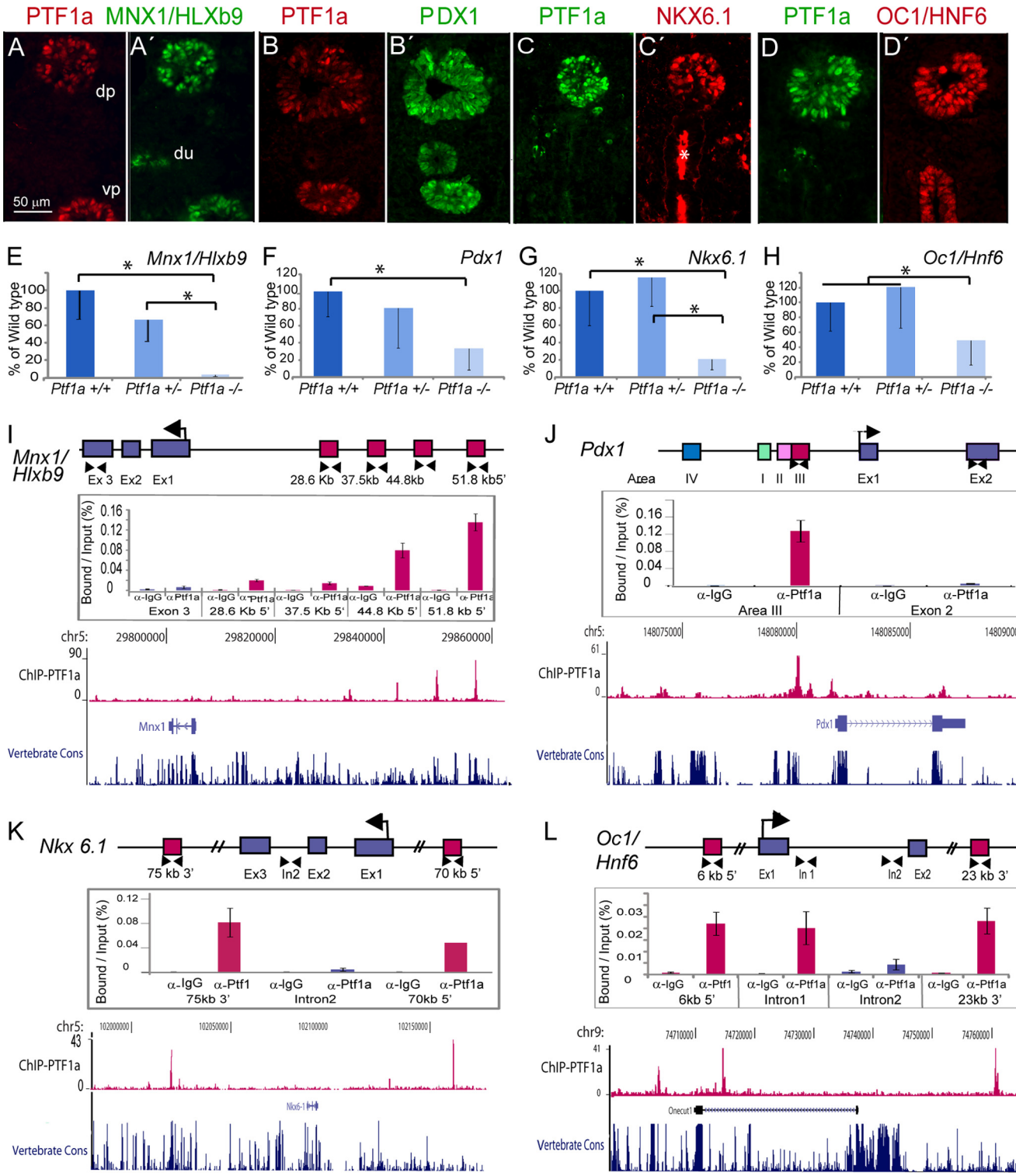

FIG 3 Four pancreatic progenitor transcription factors are direct PTF1a targets. The top panels show double immunohistochemistry with antibodies directed against PTF1a (A to D) and either MNX1 (A′), PDX1 (B′), NKX6.1 (C′) or OC1 (D′) on WT pancreas at E10.5. The same section is shown in A and A′, B and B′, C and C′, D and D′. Scale bar = 50 μm. *denotes unspecific staining in gut lumen. (E to H) Decrease in expression detected by qRT-PCR in E10.5 *Ptf1a*$^{-/-}$ compared to *Ptf1a*$^{+/-}$ and *Ptf1a*$^{+/+}$ for each of the 4 transcription factors. $n = 3$ to 4 pools of 3 buds for each genotype. Statistical significance was tested by nonparametric Mann-Whitney test. $* P < 0.05$. Scale bar = 200 μm for B and C. (I to L) Peaks of sequences enriched upon PTF1a ChIP. The ChIP-Seq peaks are aligned with the UCSC genome browser v37 on the gene loci, and the conservation of the region among vertebrates is aligned. The color-coded primers used to independently validate the bound regions by QPCR are shown with arrowheads below the gene structure. The pink boxes show areas of PTF1a binding. For each gene, a control unbound region in the locus is shown to demonstrate the specificity of peak binding as well as anti-IgG ChIP control.

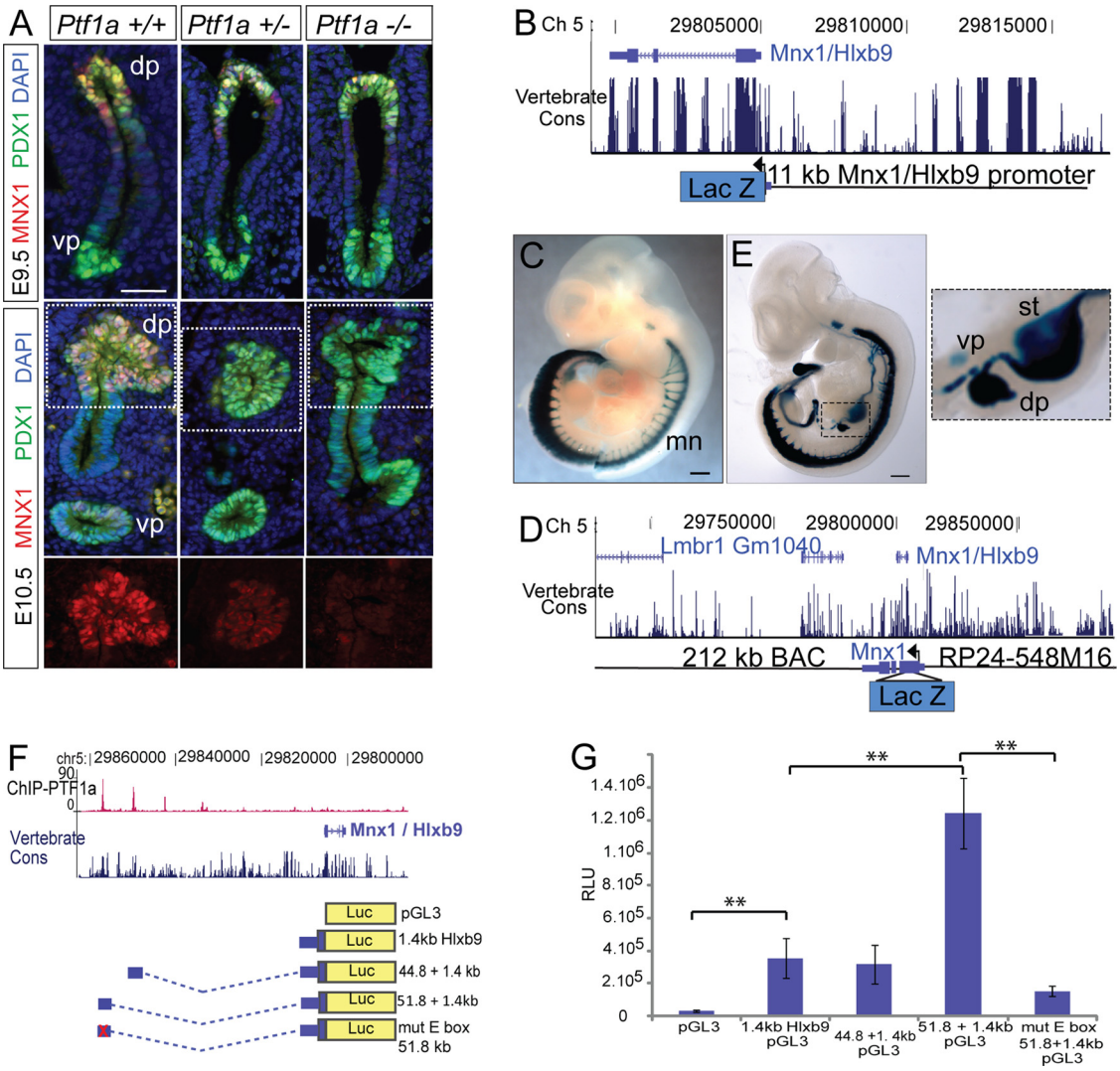

FIG 4 PTF1a is a major *Mnx1* activator through a distant enhancer. (A) Immunohistochemistry with anti-PDX1 (green) and anti-MNX1 (red) antibodies at E9.5 and E10.5. The same exposure time was used for $Ptf1a^{+/+}$, $ptf1a^{+/-}$, and $ptf1a^{-/-}$ littermates and reveals reduced MNX1 expression in the dorsal bud of $Ptf1a^{+/-}$ at E10.5. The reduction is even more drastic in KO dorsal (dp) and ventral (vp) pancreatic buds. Insets show MNX1 only in the dorsal pancreas. Scale bar = 50 μm. (B) A map of the 11-kb reporter construct is aligned with conserved sequences. (C) The 11-kb reporter introduced in transgenic mice recapitulates expression in motor neurons and hindgut but not in the pancreas. Scale bar in C and E = 100 μm. (D) A map of the 212-kb BAC reporter construct is aligned with conserved sequences. (E) The 212-kb BAC reporter introduced in transgenic mice recapitulates expression in motor neurons (mn) and hindgut as well as in the entire dorsal gut tube, including the pancreas. The posterior foregut is shown as an inset, including stomach (st), dorsal (dp), and ventral (vp) pancreas. (F) Luciferase reporter constructs in which the Mnx1 minimal promoter (1.4 kb) was associated or not with distant enhancer elements. X marks a mutation introduced in the PTF1a consensus sequence of the kb −51.8 enhancer. (G) Relative luciferase activity (RLU) in a transcriptional activity assay in which these constructs are transfected into 266-6 cells. The kb −51.8 enhancer increases activity and loses this ability upon mutation of the PTF1a consensus element. Statistical significance was tested by nonparametric Mann-Whitney test. **, $P < 0.005$.

expressed in acinar cells at E14.5 (Fig. 5A) and therefore form a synexpression group with *Ptf1a*. RHOV (or Chp for cdc42-homologous protein) is a small GTPase of the cdc42 family (5) that is crucial for neural crest specification (19). Two PTF1a binding peaks were identified by ChIP-Seq, one in the proximal promoter and one 6 kb upstream (Fig. 5B). P2RX1 is an ATP-gated nonselective ion channel. Based on *P2rx1* expression in pancreas progenitors, we investigated whether *P2rx1* KO mice (43) had a defect associated with pancreas progenitors. However, mice sacrificed at birth revealed no difference in pancreas mass and histology. P2RX1 may therefore either have redundant functions with other P2X receptors or only have postnatal functions. *P2rx1* is expected to be a direct target of PTF1a, as a single binding peak was identified in an intron or in the proximal promoter of an alternatively spliced gene. The third PTF1a-dependent gene was BMP7. Two PTF1a binding peaks were detected in *Bmp7* introns by ChIP-Seq (Fig. 5B). In an independent study investigating the function of BMPs in pancreas development, we show that BMP7 KO mice have a reduction in pancreas size at E18.5 (Gésina et al., unpublished data). As this reduction similarly affects the exocrine as well as the endocrine compartment, BMP7 may affect pancreas progenitor expansion. However, the normal size quantified at E14.5 makes it unlikely that it exerts this function via its expression in progenitors. NR5A2 is a nuclear hormone receptor that has multiple functions in development

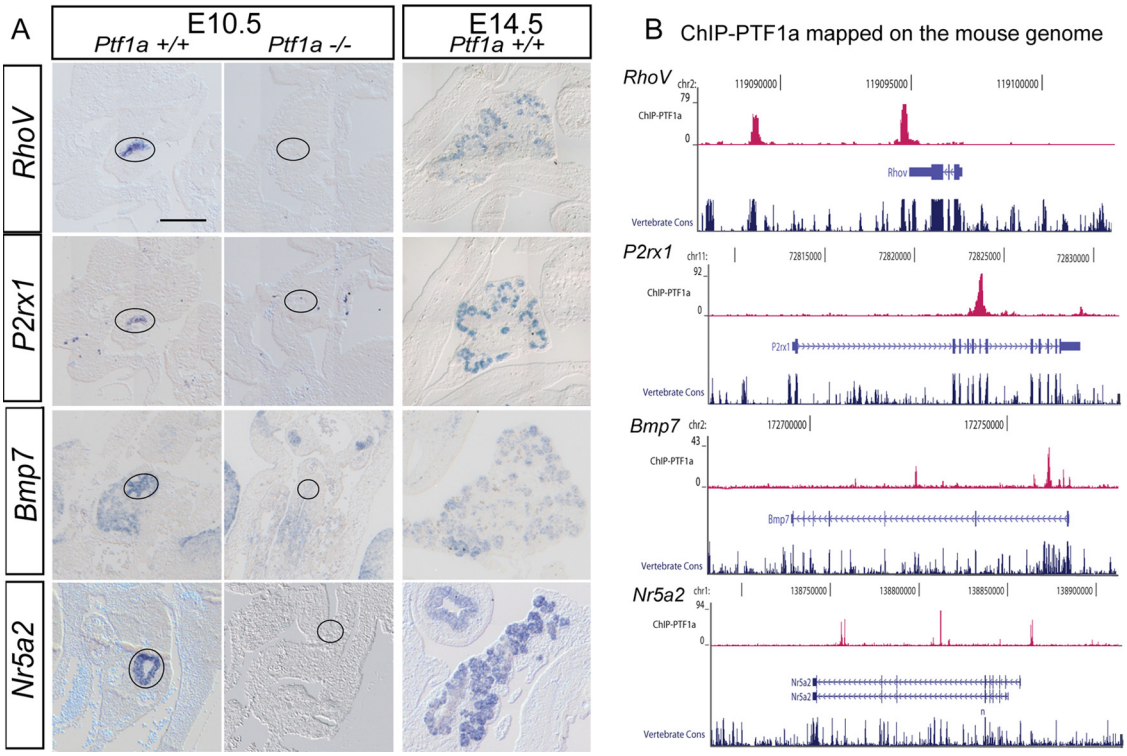

FIG 5 New PTF1a targets. (A) *In situ* hybridization with *RhoV*, *P2rx1*, *BMP7*, or *Nr5a2* probes (blue) in E10.5 *Ptf1a*$^{+/+}$ and *Ptf1a*$^{-/-}$ pancreata. Scale bar = 200 μm. This reveals a strong decrease of expression in *Ptf1a* KO. The pancreatic bud is systematically identified on an adjacent section stained with anti-Pdx1. These genes are also expressed in terminal end buds which contain exocrine cells expressing PTF1a at E14.5. (B) The four boxes show the peaks of sequences enriched upon PTF1a ChIP-Seq. The peaks are aligned with the UCSC genome browser on the gene loci, and the conservation of the region among vertebrates is aligned. One or multiple PTF1a binding peaks are revealed in the vicinity of each of these genes.

and physiology, notably in the digestive tract. In the pancreas Nr5a2 is expressed from the beginning of development and is retained in exocrine cells (3) (Fig. 5A). Its expression was previously shown to be regulated by other pancreatic transcription factors such as PDX1 (3). Although PDX1 can regulate *Nr5a2* by binding 3 elements in the 2-kb upstream sequences, we find that PTF1a directly binds 2 sites in the introns of *Nr5a2* and one closely located 3′ site (Fig. 5B). There is, therefore, most likely no clustered binding of the pancreas progenitor transcription factors driving its expression. NR5A2 was recently shown to be in a complex with PTF1a which may constitute a feed-forward activation loop (23).

DISCUSSION

Ptf1a activates many targets harboring conserved motifs, often very distant from the start site. Taken together, our results show that PTF1a regulates the expression of a wide range of targets in pancreas progenitors. Investigations in the 266-6 pancreas cell line, which expresses all pancreas progenitor markers tested, show that most of these targets are potentially directly regulated. We show that the majority of direct targets exhibit an E-box and RBPJ binding sequences 1, 2, or 3 helix turns apart within the binding peaks. The presence of an E-box and A/TC-box sequences with such spacing has a predictive value of binding of 50%, which is unusually high, especially bearing in mind that the ChIP-Seq was performed on only one cell line and PTF1a may have other targets in other tissues such as the nervous system. The binding and regulation in other tissues where PTF1a is expressed, such as the exocrine cells of the pancreas (40), the retina, cerebellum, and spinal cord, will be important to clarify the correlation between regulated genes and bound sequences. The absence of peaks within 50 kb of the genes upregulated in *Ptf1a* KO makes it unlikely that it acts as a repressor in the context under study. Our experiments also reveal that PTF1a binding sites can be very distant from genes. The observation that pancreas expression of *Mnx1* requires distant elements suggests that the distant binding sites are functionally important.

Ptf1a is a major direct regulator of *Mnx1* expression. Our experiments show that PTF1a is necessary to maintain the expression of multiple transcription factors previously shown to be essential for pancreas progenitor identity emergence and maintenance. Among those, the gene that relies most heavily upon PTF1a for its expression is *Mnx1/Hlxb9*. *Mnx1/Hlxb9* is essential for the formation of the dorsal pancreatic bud (21, 35). Since *Mnx1/Hlxb9* is also expressed in the notochord, conditional inactivation will be important to investigate its direct activities in pancreas progenitors. Although restoration of MNX1 in *Ptf1a* KOs would clarify to what extent PTF1a activities in pancreas progenitors are mediated by MNX1, the experiment is unfortunately impossible as MNX1 gain-of-function in the pancreas leads to aberrant development (36). Of interest, after E11.5, PTF1a is upregulated in terminal end buds and subsequently acinar cells whereas MNX1 expression ceases (36), suggesting that other mechanisms block *Mnx1* expression after this stage.

PTF1a more generally sustains a transcription factor network that maintains pancreas progenitors. The other transcrip-

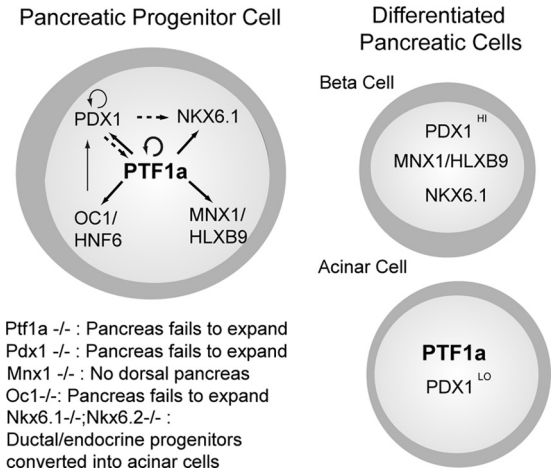

FIG 6 Transcription factor network which maintains pancreas progenitors.

tion factors that are regulated by PTF1a are *Pdx1* (28, 47), *OC1/Hnf6* (25), *Nkx6.1* (8, 56), and itself (Fig. 6, strong black arrows showing the targets identified here). This is most likely done through direct binding to their regulatory sequences. Several cross-regulatory interactions have been previously reported between the genes we identify downstream of PTF1a, thereby stabilizing pancreas identity. RNA profiling of *Pdx1* KO versus WT has shown that PDX1 is needed, directly or not, for *Ptf1a* and *Nkx6.1* expression (Fig. 6, dashed arrows) (51, 61). Pdx1 maintains its own expression (10). OC1/HNF6 directly activates *Pdx1* promoter (25) (Fig. 6, previous direct targets, thin black arrows) The onset of PTF1a expression after PDX1 and MNX1 suggests that PTF1a stabilizes rather than initiates the network. This network contains at least two autoregulatory loops (*Pdx1* and *Ptf1a*) and one feed-forward loop (between *Pdx1* and *Ptf1a*) which all tend to promote robustness of states. This network is, however, very easily destabilized, as the KO of any component (but the repressor NKX6.1) leads to pancreas bud collapse. Other genes initiating *Ptf1a* expression remain to be discovered as *Pdx1*, more widely expressed than *Ptf1a*, is clearly not sufficient to promote *Ptf1a* expression. In contrast to our observations, PTF1a was shown to downregulate NKX6.1 at E14.5, based on gain-of-function experiments (56), highlighting that the network downstream of PTF1a changes with time and context. PTF1a being expected to be a transcriptional activator suggests that the late inhibitory mechanism is indirect and it may employ a relay factor not present at E10.5. The relationship between *Nkx6.1* and *Ptf1a*, initially coexpressed and subsequently mutually exclusive, could constitute a negative feedback loop leading to the segregation of the early pancreas progenitor domain into exocrine and centrally located multipotent progenitor domain (see also references 8 and 56). A general catalogue of PDX1, MNX1, OC1, and NKX6.1 targets would be useful to better understand the pancreas progenitor network more completely. In addition, other signal inputs such as Fgf10 and Notch signaling, which induces Pdx1 (7, 22, 26, 45), and a putative blood vessel signal inducing Ptf1a (33, 64) are likely to play an important role in the network.

Four new PTF1a targets. Our experiments were used to identify new direct PTF1a targets which may be used as markers of pancreas progenitors and exocrine cells. Among those, two were previously known to be expressed in pancreas progenitors (*Bmp7* and *Nr5a2*) and two were known only in other organs (*RhoV* and *P2rx1*). These genes share the same expression pattern as *Ptf1a* in the pancreas, initially in progenitors and subsequently in exocrine cells, suggesting that the regulation of their expression receives strong inputs from PTF1a. However, their expression in other organs devoid of *Ptf1a* expression suggests multiple regulatory inputs. Our functional investigations show that *P2rx1* is not needed for pancreas progenitor maintenance or their differentiation into exocrine and endocrine cells but do not exclude a later role in exocrine cells. Similarly, our studies of *Bmp7* knockout mice show that *Bmp7* regulates pancreas expansion but only at a stage where it is expressed in the acinar cell-committed terminal end buds. This raises the hypothesis that these and several other PTF1a targets may be turned on by PTF1a in progenitors without a functional role. Although the function of *RhoV* and *Nr5a2* during development was not investigated, a crucial function of *Nr5a2* was recently reported in adult exocrine cells. Interestingly, NR5A2 controls multiple exocrine targets by forming a complex with PTF1a. Since we show that PTF1a directly binds the NR5A2 promoter, this may constitute a feed-forward loop.

A better knowledge of the transcriptional network operating in pancreas progenitors will be useful to identify combinations of transcription factors that may self-entrain the network and thereby trigger the maintenance and expansion of pancreas progenitors. Such progenitors can be produced from embryonic stem cells and have the potential to then differentiate into β-cells for clinical applications in diabetes.

ACKNOWLEDGMENTS

This work was funded by Juvenile Diabetes Research Foundation grant 1-2006-606.

We are grateful to Peter Wellauer for transmitting his interest and knowledge about PTF1. We thank Bernadette Bréant and Chris Wright for sharing the PTF1a and Pdx1 antibodies for immunohistochemistry, Daniel Graf for BMP7 KO tissue and sharing information, and Richard Evan for sharing *P2rx1* KO mice. We thank the numerous people who had inputs into ChIP, more particularly Sunil Raghav and the Lausanne Genomics Technologies Facility (GTF) for their excellent support. We are grateful to Otto Hagenbüchle and Tatiana Petrova for comments on the manuscript.

N.T., E.G., P.B., and A.G.B. designed experiments and wrote the manuscript. N.T. performed all experiments but those referred to below. E.G. investigated target genes by ISH and characterized the phenotype of *P2rx1* and *Bmp7* KO mice. P.S. amplified cDNA for expression profiling. P.B. performed the bioinformatics analysis of ChIP-Seq data.

REFERENCES

1. **Afelik S, Chen Y, Pieler T.** 2006. Combined ectopic expression of Pdx1 and Ptf1a/p48 results in the stable conversion of posterior endoderm into endocrine and exocrine pancreatic tissue. Genes Dev. **20**:1441–1446.
2. **Aldinger KA, Elsen GE.** 2008. Ptf1a is a molecular determinant for both glutamatergic and GABAergic neurons in the hindbrain. J. Neurosci. **28**: 338–339.
3. **Annicotte JS, et al.** 2003. Pancreatic-duodenal homeobox 1 regulates expression of liver receptor homolog 1 during pancreas development. Mol. Cell. Biol. **23**:6713–6724.
4. **Arber S, et al.** 1999. Requirement for the homeobox gene Hb9 in the consolidation of motor neuron identity. Neuron **23**:659–674.
5. **Aronheim A, et al.** 1998. Chp, a homologue of the GTPase Cdc42Hs, activates the JNK pathway and is implicated in reorganizing the actin cytoskeleton. Curr. Biol. **8**:1125–1128.
6. **Beres TM, et al.** 2006. PTF1 is an organ-specific and notch-independent basic helix-loop-helix complex containing the mammalian suppressor of hairless (RBP-J) or its paralogue, RBP-L. Mol. Cell. Biol. **26**:117–130.

7. **Bhushan A, et al.** 2001. Fgf10 is essential for maintaining the proliferative capacity of epithelial progenitor cells during early pancreatic organogenesis. Development **128**:5109–5117.
8. **Binot AC, et al.** 2010. nkx6.1 and nkx6.2 regulate alpha- and beta-cell formation in zebrafish by acting on pancreatic endocrine progenitor cells. Dev. Biol. **340**:397–407.
9. **Burlison JS, Long Q, Fujitani Y, Wright CV, Magnuson MA.** 2008. Pdx-1 and Ptf1a concurrently determine fate specification of pancreatic multipotent progenitor cells. Dev. Biol. **316**:74–86.
10. **Chakrabarti SK, James JC, Mirmira RG.** 2002. Quantitative assessment of gene targeting in vitro and in vivo by the pancreatic transcription factor, Pdx1. Importance of chromatin structure in directing promoter binding. J. Biol. Chem. **277**:13286–13293.
11. **Cockell M, Stevenson BJ, Strubin M, Hagenbuchle O, Wellauer PK.** 1989. Identification of a cell-specific DNA-binding activity that interacts with a transcriptional activator of genes expressed in the acinar pancreas. Mol. Cell. Biol. **9**:2464–2476.
12. **Dennis G, Jr, et al.** 2003. DAVID: database for annotation, visualization, and integrated discovery. Genome Biol. **4**:P3.
13. **Dong PD, Provost E, Leach SD, Stainier DY.** 2008. Graded levels of Ptf1a differentially regulate endocrine and exocrine fates in the developing pancreas. Genes Dev. **22**:1445–1450.
14. **Dullin JP, et al.** 2007. Ptf1a triggers GABAergic neuronal cell fates in the retina. BMC Dev. Biol. **7**:110.
15. **Fujitani Y, et al.** 2006. Ptf1a determines horizontal and amacrine cell fates during mouse retinal development. Development **133**:4439–4450.
16. **Fukuda A, et al.** 2008. Reduction of Ptf1a gene dosage causes pancreatic hypoplasia and diabetes in mice. Diabetes **57**:2421–2431.
17. **Gao N, et al.** 2008. Dynamic regulation of Pdx1 enhancers by Foxa1 and Foxa2 is essential for pancreas development. Genes Dev. **22**:3435–3448.
18. **Glasgow SM, Henke RM, Macdonald RJ, Wright CV, Johnson JE.** 2005. Ptf1a determines GABAergic over glutamatergic neuronal cell fate in the spinal cord dorsal horn. Development **132**:5461–5469.
19. **Guémar L, et al.** 2007. The small GTPase RhoV is an essential regulator of neural crest induction in Xenopus. Dev. Biol. **310**:113–128.
20. **Hald J, et al.** 2008. Generation and characterization of Ptf1a antiserum and localization of Ptf1a in relation to Nkx6.1 and Pdx1 during the earliest stages of mouse pancreas development. J. Histochem. Cytochem. **56**:587–595.
21. **Harrison KA, Thaler J, Pfaff SL, Gu H, Kehrl JH.** 1999. Pancreas dorsal lobe agenesis and abnormal islets of Langerhans in Hlxb9-deficient mice. Nat. Genet. **23**:71–75.
22. **Hart A, Papadopoulou S, Edlund H.** 2003. Fgf10 maintains notch activation, stimulates proliferation, and blocks differentiation of pancreatic epithelial cells. Dev. Dyn. **228**:185–193.
23. **Holmstrom SR, et al.** 2011. LRH-1 and PTF1-L coregulate an exocrine pancreas-specific transcriptional network for digestive function. Genes Dev. **25**:1674–1679.
24. **Hoshino M, et al.** 2005. Ptf1a, a bHLH transcriptional gene, defines GABAergic neuronal fates in cerebellum. Neuron **47**:201–213.
25. **Jacquemin P, Lemaigre FP, Rousseau GG.** 2003. The Onecut transcription factor HNF-6 (OC-1) is required for timely specification of the pancreas and acts upstream of Pdx-1 in the specification cascade. Dev. Biol. **258**:105–116.
26. **Jacquemin P, et al.** 2006. An endothelial-mesenchymal relay pathway regulates early phases of pancreas development. Dev. Biol. **290**:189–199.
27. **Jarikji ZH, et al.** 2007. Differential ability of Ptf1a and Ptf1a-VP16 to convert stomach, duodenum and liver to pancreas. Dev. Biol. **304**:786–799.
28. **Jonsson J, Carlsson L, Edlund T, Edlund H.** 1994. Insulin-promoter-factor 1 is required for pancreas development in mice. Nature **371**:606–609.
29. **Kawaguchi Y, et al.** 2002. The role of the transcriptional regulator Ptf1a in converting intestinal to pancreatic progenitors. Nat. Genet. **32**:128–134.
30. **Kent WJ, Zweig AS, Barber G, Hinrichs AS, Karolchik D.** 2010. BigWig and BigBed: enabling browsing of large distributed datasets. Bioinformatics **26**:2204–2207.
31. **Krapp A, et al.** 1996. The p48 DNA-binding subunit of transcription factor PTF1 is a new exocrine pancreas-specific basic helix-loop-helix protein. EMBO J. **15**:4317–4329.
32. **Krapp A, et al.** 1998. The bHLH protein PTF1-p48 is essential for the formation of the exocrine and the correct spatial organization of the endocrine pancreas. Genes Dev. **12**:3752–3763.
33. **Lammert E, Cleaver O, Melton D.** 2001. Induction of pancreatic differentiation by signals from blood vessels. Science **294**:564–567.
34. **Lee SK, Jurata LW, Funahashi J, Ruiz EC, Pfaff SL.** 2004. Analysis of embryonic motoneuron gene regulation: derepression of general activators function in concert with enhancer factors. Development **131**:3295–3306.
35. **Li H, Arber S, Jessell TM, Edlund H.** 1999. Selective agenesis of the dorsal pancreas in mice lacking homeobox gene Hlxb9. Nat. Genet. **23**:67–70.
36. **Li H, Edlund H.** 2001. Persistent expression of Hlxb9 in the pancreatic epithelium impairs pancreatic development. Dev. Biol. **240**:247–253.
37. **Li Z, et al.** 2003. A global transcriptional regulatory role for c-Myc in Burkitt's lymphoma cells. Proc. Natl. Acad. Sci. U. S. A. **100**:8164–8169.
38. **Lin JW, et al.** 2004. Differential requirement for ptf1a in endocrine and exocrine lineages of developing zebrafish pancreas. Dev. Biol. **274**:491–503.
39. **Masui T, Long Q, Beres TM, Magnuson MA, MacDonald RJ.** 2007. Early pancreatic development requires the vertebrate Suppressor of Hairless (RBPJ) in the PTF1 bHLH complex. Genes Dev. **21**:2629–2643.
40. **Masui T, et al.** 2010. Replacement of Rbpj with Rbpjl in the PTF1 complex controls the final maturation of pancreatic acinar cells. Gastroenterology **139**:270–280.
41. **Masui T, et al.** 2008. Transcriptional autoregulation controls pancreatic Ptf1a expression during development and adulthood. Mol. Cell. Biol. **28**:5458–5468.
42. **Miyatsuka T, et al.** 2007. Ptf1a and RBP-J cooperate in activating Pdx1 gene expression through binding to area III. Biochem. Biophys. Res. Commun. **362**:905–909.
43. **Mulryan K, et al.** 2000. Reduced vas deferens contraction and male infertility in mice lacking P2X1 receptors. Nature **403**:86–89.
44. **Nakhai H, et al.** 2007. Ptf1a is essential for the differentiation of GABAergic and glycinergic amacrine cells and horizontal cells in the mouse retina. Development **134**:1151–1160.
45. **Norgaard GA, Jensen JN, Jensen J.** 2003. FGF10 signaling maintains the pancreatic progenitor cell state revealing a novel role of Notch in organ development. Dev. Biol. **264**:323–338.
46. **Obata J, et al.** 2001. p48 subunit of mouse PTF1 binds to RBP-Jkappa/CBF-1, the intracellular mediator of Notch signalling, and is expressed in the neural tube of early stage embryos. Genes Cells **6**:345–360.
47. **Offield MF, et al.** 1996. PDX-1 is required for pancreatic outgrowth and differentiation of the rostral duodenum. Development **122**:983–995.
48. **Ornitz DM, et al.** 1985. Specific expression of an elastase-human growth hormone fusion gene in pancreatic acinar cells of transgenic mice. Nature **313**:600–602.
49. **Ornitz DM, et al.** 1985. Elastase I promoter directs expression of human growth hormone and SV40 T antigen genes to pancreatic acinar cells in transgenic mice. Cold Spring Harb. Symp. Quant. Biol. **50**:399–409.
50. **Pascual M, et al.** 2007. Cerebellar GABAergic progenitors adopt an external granule cell-like phenotype in the absence of Ptf1a transcription factor expression. Proc. Natl. Acad. Sci. U. S. A. **104**:5193–5198.
51. **Pedersen JK, et al.** 2005. Endodermal expression of Nkx6 genes depends differently on Pdx1. Dev. Biol. **288**:487–501.
52. **Psarros M, et al.** 2005. RACE: remote analysis computation for gene expression data. Nucleic Acids Res. **33**:W638–W643.
53. **Rose SD, Kruse F, Swift GH, MacDonald RJ, Hammer RE.** 1994. A single element of the elastase I enhancer is sufficient to direct transcription selectively to the pancreas and gut. Mol. Cell. Biol. **14**:2048–2057.
54. **Rose SD, Swift GH, Peyton MJ, Hammer RE, MacDonald RJ.** 2001. The role of PTF1-P48 in pancreatic acinar gene expression. J. Biol. Chem. **276**:44018–44026.
55. **Roux E, Strubin M, Hagenbuchle O, Wellauer PK.** 1989. The cell-specific transcription factor PTF1 contains two different subunits that interact with the DNA. Genes Dev. **3**:1613–1624.
56. **Schaffer AE, Freude KK, Nelson SB, Sander M.** 2010. Nkx6 transcription factors and Ptf1a function as antagonistic lineage determinants in multipotent pancreatic progenitors. Dev. Cell **18**:1022–1029.
57. **Schmid CD, Bucher P.** 2010. MER41 repeat sequences contain inducible STAT1 binding sites. PLoS One **5**:e11425.
58. **Sellick GS, et al.** 2004. Mutations in PTF1A cause pancreatic and cerebellar agenesis. Nat. Genet. **36**:1301–1305.
59. **Sellick GS, Garrett C, Houlston RS.** 2003. A novel gene for neonatal diabetes maps to chromosome 10p12.1-p13. Diabetes **52**:2636–2638.
60. **Sommer L, Hagenbuchle O, Wellauer PK, Strubin M.** 1991. Nuclear

targeting of the transcription factor PTF1 is mediated by a protein subunit that does not bind to the PTF1 cognate sequence. Cell **67**:987–994.
61. **Svensson P, et al.** 2007. Gene array identification of Ipf1/Pdx1−/− regulated genes in pancreatic progenitor cells. BMC Dev. Biol. **7**:129.
62. **Tutak E, et al.** 2009. A Turkish newborn infant with cerebellar agenesis/neonatal diabetes mellitus and PTF1A mutation. Genet. Couns. **20**:147–152.
63. **Wiebe PO, et al.** 2007. Ptf1a binds to and activates area III, a highly conserved region of the Pdx1 promoter that mediates early pancreas-wide Pdx1 expression. Mol. Cell. Biol. **27**:4093–4104.
64. **Yoshitomi H, Zaret KS.** 2004. Endothelial cell interactions initiate dorsal pancreas development by selectively inducing the transcription factor Ptf1a. Development **131**:807–817.
65. **Zhou Q, et al.** 2007. A multipotent progenitor domain guides pancreatic organogenesis. Dev. Cell **13**:103–114.